

Sediment Transport at Density Fronts in Shallow Water

David K. Ralston
Applied Ocean Physics and Engineering, MS #12
Woods Hole, MA 02543
phone: (508) 289-2587 fax: (508) 457-2194 email: dralston@whoi.edu

Award Number: N00014-08-1-0846

LONG-TERM GOALS

The goal of this research is to quantify through observations and modeling how density fronts in shallow estuarine flows impact the mobilization, redistribution, trapping, and deposition of suspended sediment.

OBJECTIVES

The objectives of this research program are to

- implement a high-resolution, 3-dimensional, finite-volume hydrodynamic model of tidal flats field site including advanced sediment transport algorithms,
- integrate and test a set of field instruments to measure density, velocity, and suspended sediment concentration at density fronts in shallow water (< 1 m),
- characterize flow and suspended sediment at a density front through the tidal inundation cycle as it travels across the intertidal zone, and
- combine the observations and model results to (1) quantify sediment suspension, trapping, and circulation at the front, (2) determine effects of frontal sediment transport on the net sediment fluxes in shallow estuarine settings, and (3) evaluate and improve the sediment transport model.

APPROACH

The research approach combines observational and modeling techniques. In the field, we measured velocity and suspended sediment at high resolution in shallow flows, tracking the evolution of the salinity front through the tidal cycle. The instrumentation incorporated an acoustic Doppler current profiler (ADCP) to measure currents and a profiling conductivity-temperature-depth sensor (CTD) to measure water column salinity and density. Suspended sediment concentrations were based on a combination of acoustic and optical sensors, with calibration provided by gravimetric analysis of water samples taken during the surveys. A major field effort occurred in June 2009 on the Skagit Tidal flats in Puget Sound, coordinated with other researchers in the Tidal Flats DRI. Focused, Lagrangian observations of the shallow density front and its evolution through the tidal cycle were complemented by a large scale array of moored instruments deployed during the same period (along with Geyer and Traykovski).

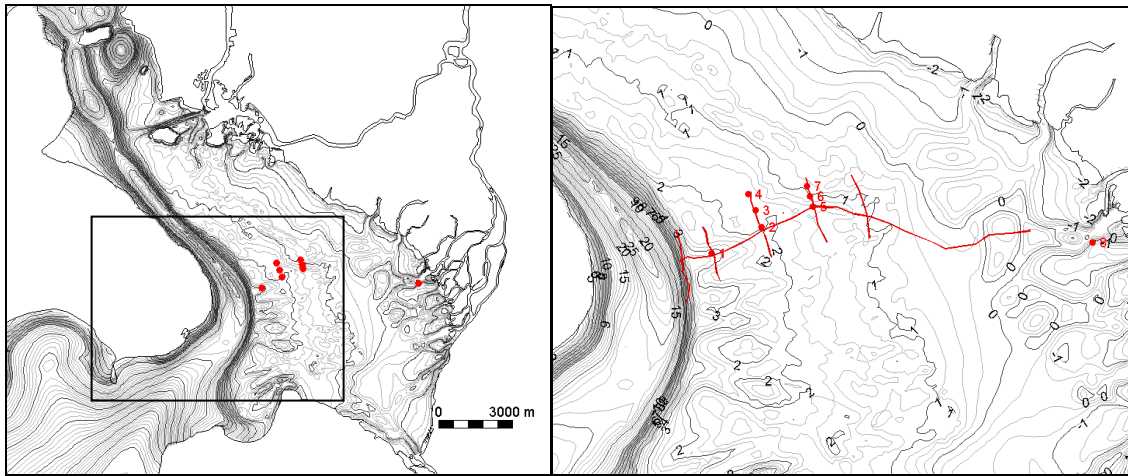


Figure 1. Bathymetry of the Skagit Bay tidal flats (left) with a zoom on the study area on the southern flats (right). Red dots indicate frame locations and lines show across-flats and across-channel survey lines.

In parallel with the observations, we developed a numerical model of the Skagit tidal flats. The model uses the Finite Volume Coastal Ocean Model (FVCOM), but was modified to incorporate recent advancements in sediment transport modeling with the Community Sediment Transport Model System (CSTMS). The unstructured grid of FVCOM allows the model to simulate conditions the Skagit flats with enhanced grid resolution near the observations. The observations were used to calibrate the model and to evaluate how well the model represents sharp salinity gradients at fronts, both across the tidal flats and at lateral fronts coinciding with channel-shoal bathymetry. Collectively, analyses of the observations and model were used to quantify how local frontal processes on scales of 10's to 100's of meters impact retention, redistribution, and export of sediment over tidal flats on scales of kilometers.

WORK COMPLETED

A major field effort was conducted in June 2009. We deployed an array of instruments on the Skagit flats (Fig. 1) to measure the flow and sediment-transport. After deployment and just before recovery, we conducted high-resolution surveys of the currents, density, and suspended sediment distributions on the flats over multiple tidal cycles. Surveys (locations shown in Fig. 1) were designed to characterize the cross-flat structure of the salinity front, and how the lateral distribution of density, currents, and suspended sediment depended on the structure of distributary channels on the flats. Instruments at the quadpod stations measured acoustic profiles and optical point measurements of suspended sediment, bed elevation, horizontal and vertical velocity, conductivity, temperature and depth. The acoustic profiles of sediment concentration and bed elevation were measured with Acoustic Backscatter Sensors (ABSs) and Pulse Coherent Doppler profilers. Each of the pods had 1 or 2 near-bed Acoustic Doppler Velocimeters (ADV) for tidal currents, waves and turbulence. The stations had accompanying surface moorings with TS/OBS sensors, to quantify vertical and horizontal salinity and sediment gradients.

Extensive efforts went into development of a high-resolution numerical of the Skagit tidal flats and surrounding region. Bathymetry was collected from multiple sources and combined to create an unstructured grid (Figure 2). Grid resolution ranged from about 10 m on the flats to over 500 m in more distant parts of the domain. The bathymetry and grid in the distributary network of the Skagit

were refined based on surveys of depth and discharge in the river during the June 2009 observations. Additional bathymetric data were acquired from other investigators – jet ski surveys near the mouth of the North Fork (Raubenheimer and Elgar, WHOI) and aircraft surveys using LiDAR of the most of the intertidal region (Brozena, NRL).

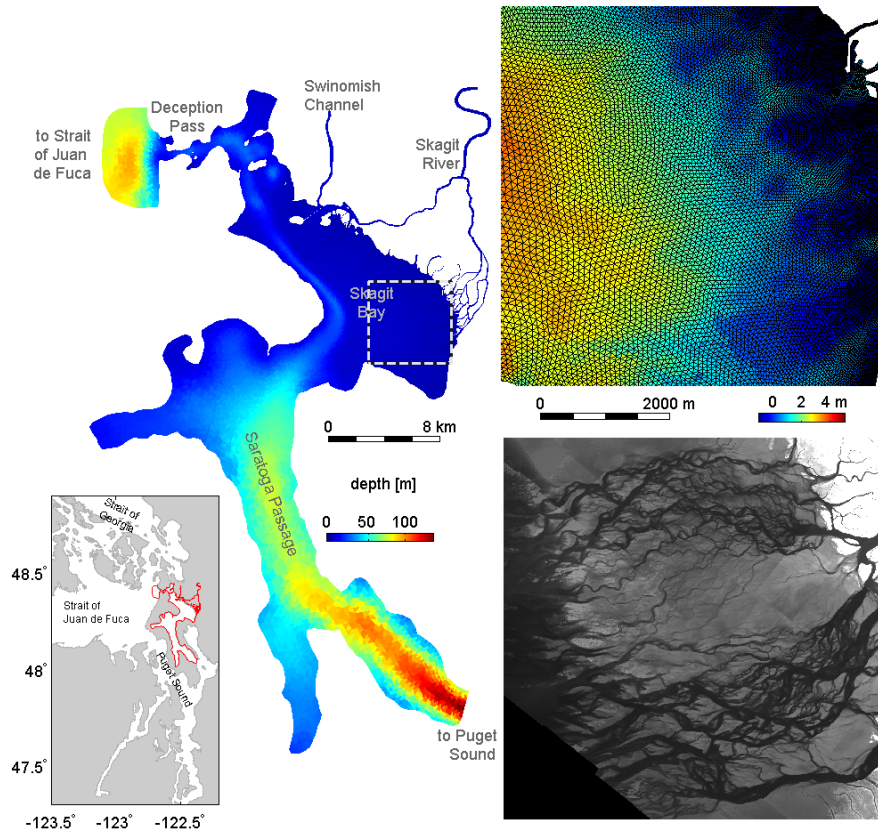


Figure 2. Model grid of Skagit flats and surrounding region: (lower left) location relative to Puget Sound and Strait of Juan de Fuca; (upper left) domain bathymetry, (upper right) zoom on southern tidal flats shown in box, with grid cells (minimum horizontal grid scale is about 10 m); (lower right) near infrared image of channels on emergent tidal flats around low tide (image courtesy K. Hooper, Artete Assoc.).

In addition to the grid and forcing, the hydrodynamic code (FVCOM) was modified and tested for this implementation. A sediment transport module using the latest version of the CSTMS was added, and simulations were run for test cases and for the Skagit domain. Initial comparisons between model results and observations suggested that local wind forcing was important for generating surface wind stress that affected mean currents and vertical mixing rates. The Skagit model was adapted to incorporate observed winds, improving model skill for salinity and velocity at stations near the wind observations. However, analysis of winds at a multiple stations in the study region indicated significant heterogeneity in the wind field due to the complex orography of Puget Sound. To address this, we developed an atmospheric model of the region using the Weather Research and Forecasting model (WRF) and coupled it to FVCOM.

Several manuscripts have been published this year based on data from the Skagit analyzed in this project. Topics included quantifying impacts of estuarine and fluvial process on sediment fluxes (Ralston et al., *CSR*, 2012), an analyses of generation mechanisms for tidal asymmetries on the tidal flats (Nidzieko and Ralston, 2012), and an evaluation of effects of complex topography on wind correlation length scales and implications for coastal ocean modeling (Raubenheimer et al., 2012).

Recently, we have extended the examination of the sediment trapping processes identified in the Skagit to other estuarine environments. We analyzed sediment transport processes in the Hudson River estuary using model results that incorporated the same CSTMS code, but within the Regional Ocean Modeling System (ROMS) circulation model instead of FVCOM. We have written a manuscript on these results, and it was recently accepted for publication (Ralston et al., *JGR*, 2012).

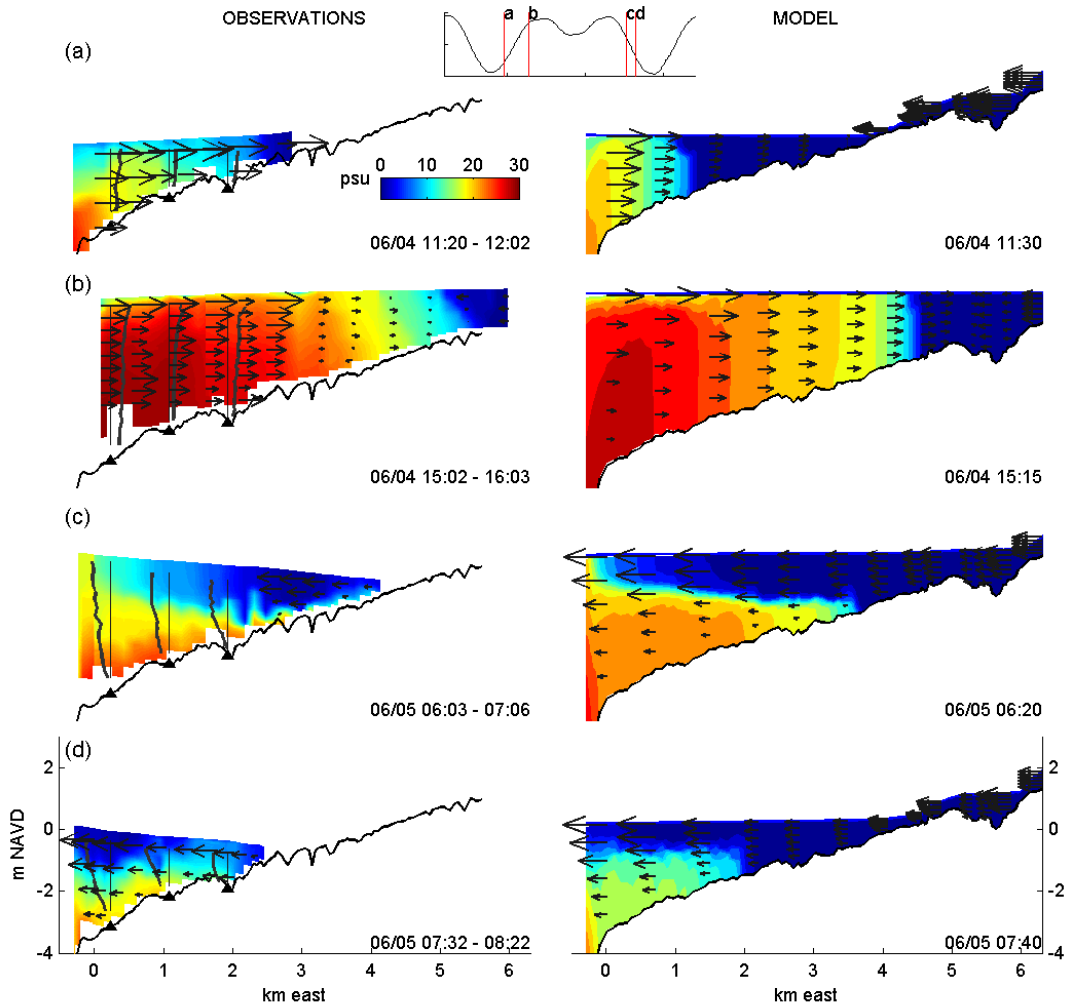


Figure 3. Across-shore transects of salinity on the Skagit flats, from observations (left) and model (right). Top 2 rows are during a flood tide, with a relatively strong horizontal salinity gradient and little stratification in the front; in both the model and observations a near surface layer of fresher water can be seen behind the front. Bottom 2 rows are during an ebb, when stratification was strong even in water as shallow as ~1 m. Location of transect is shown in Fig. 1.

RESULTS

Skagit model simulations were run with realistic forcing (tides, river discharge) corresponding with the observation period in June 2009. Comparisons between observed and model salinity, velocity, and water surface elevation were used to adjust key model parameters. An important result of the calibration was to show that low background mixing and bottom friction are needed for accurate simulations. The Skagit flats were strongly stratified at times due to the spring freshet, with river discharge ranging between $930 \text{ m}^3 \text{ s}^{-1}$ in early June and about $450 \text{ m}^3 \text{ s}^{-1}$ by the end of the month. To maintain sharp horizontal and vertical salinity gradients, the background values for turbulent and horizontal diffusivity were set to $10^{-6} \text{ m}^2 \text{ s}^{-1}$ and 0, respectively. Similarly, the bottom roughness (z_0) was set to 0.1 mm, representative of small roughness elements on the flats. One surprising result was the importance of vertical resolution for simulating the observed salinity structure on the flats. Although the shallow water depths might suggest fewer vertical levels are necessary than in models with deeper domains, the sharp vertical gradients and the relatively steep bottom topography combined with the sigma-coordinate system of FVCOM (and many similar coastal models) can lead to spurious vertical mixing. For example, model runs with 20 sigma-levels had weaker stratification on the flats, a shorter salinity intrusion, and consequently different sediment trapping than simulations with 30 levels.

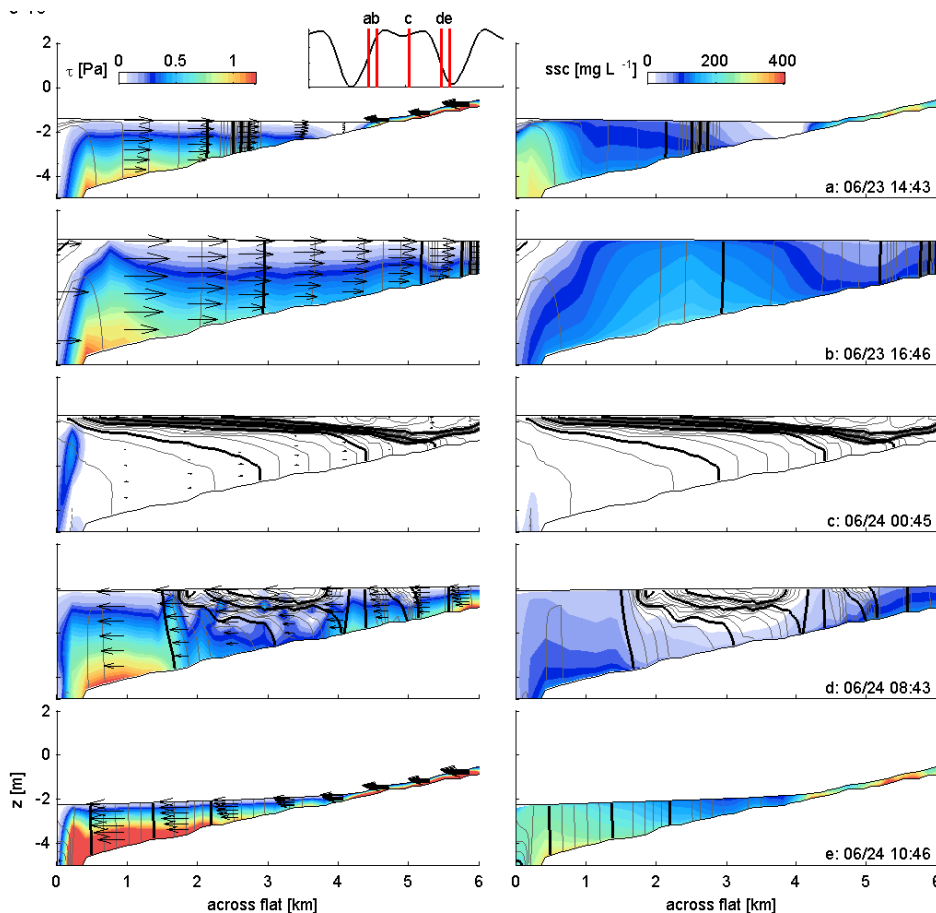


Figure 4. Across-shore transects in a channel of stress (left panels) and suspended-sediment concentration (right) from the models. Location of transect is same as in Fig. 3. Transects are from a diurnal period during spring tides, with snapshots during the large flood (top 2 rows), small ebb (middle row), and large ebb (bottom 2 rows). Salinity contours are shown, with intervals of 1 psu (thin gray) and 5 psu (thick black).

The calibrated model results compared well with the moored time series of water surface elevation, velocity, salinity and stratification, and with observations from spatial surveys (Figure 3). The model reflected the observed diurnal tidal pattern of extreme variability in stratification: unstratified during the strong floods, stratifying at high water and remaining stratified through the weaker ebb and flood, and mixing midway through the strong ebb. Similarly, comparisons with ADCP data showed that the magnitude and vertical structure of velocity were well-resolved in the model. Critically for suspended sediment transport calculations, the bed stresses calculated in the model compared well with near-bed stresses from the ADVs, including ebb-flood asymmetries. Stratification modulated the tidal stresses, with higher stresses during unstratified flood tides, and weaker stresses during stratified ebbs up until the point that stratification breaks down. Similarly, comparisons between observed (through calibrated optical and acoustic measurements) and modeled suspended sediment showed good agreement.

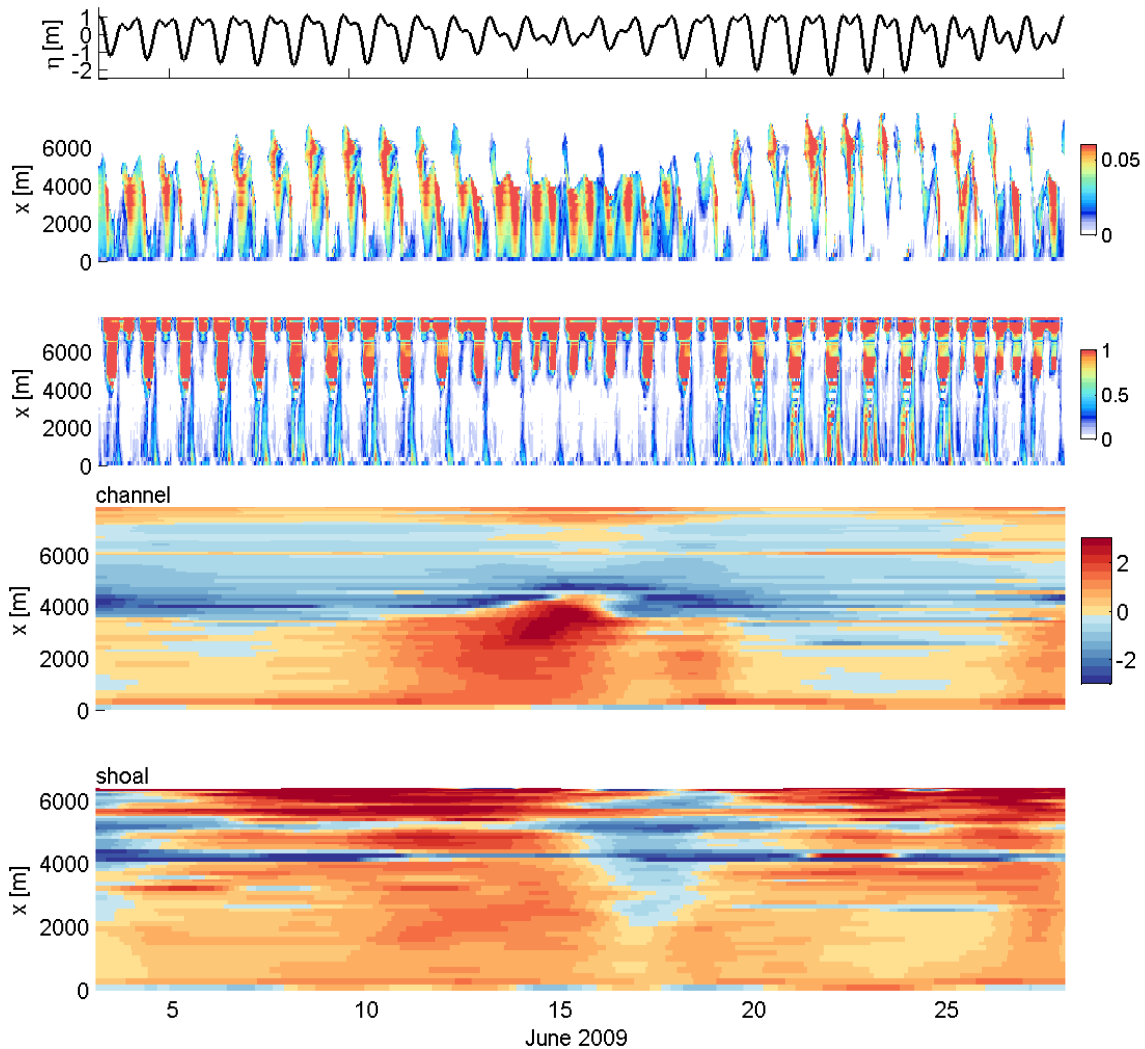


Figure 5. Model results of stratification, stress, and stress asymmetry in a section across the south Skagit tidal flats (location shown in Fig 1): [top panel] water surface elevation, [panel 2] stratification (buoyancy frequency) as a function of distance across the flats and time (s^{-2}), [panel 3] bottom stress ($N m^{-2}$), [panel 4] stress asymmetry in a tributary channel (skewness, with flood-directed asymmetry > 0 and ebb-directed < 0), [panel 5] stress asymmetry on tidal flats adjacent to the tributary channel shown in [panel 4].

An example from the model during a diurnal tidal cycle discharge illustrates the importance of stratification and baroclinicity to sediment dynamics on Skagit tidal flats (Fig 4). During the flood, the salinity front advects across the flats with a region of high stress, and correspondingly high suspended sediment concentration, in the region of weak stratification behind the front. In contrast, early in the ensuing ebb strong stratification extends over nearly the entire width of the tidal flats, so bed stresses and sediment concentrations are minimal. As the water level falls later in the ebb, the stratification is mixed away. At the grid resolution of 10 to 20 m in the study region, the model reproduces many of the features observed in cross-flat transects. Additionally, the model provides information on the spatial structure of the currents and freshwater that is not possible to measure synoptically in the field.

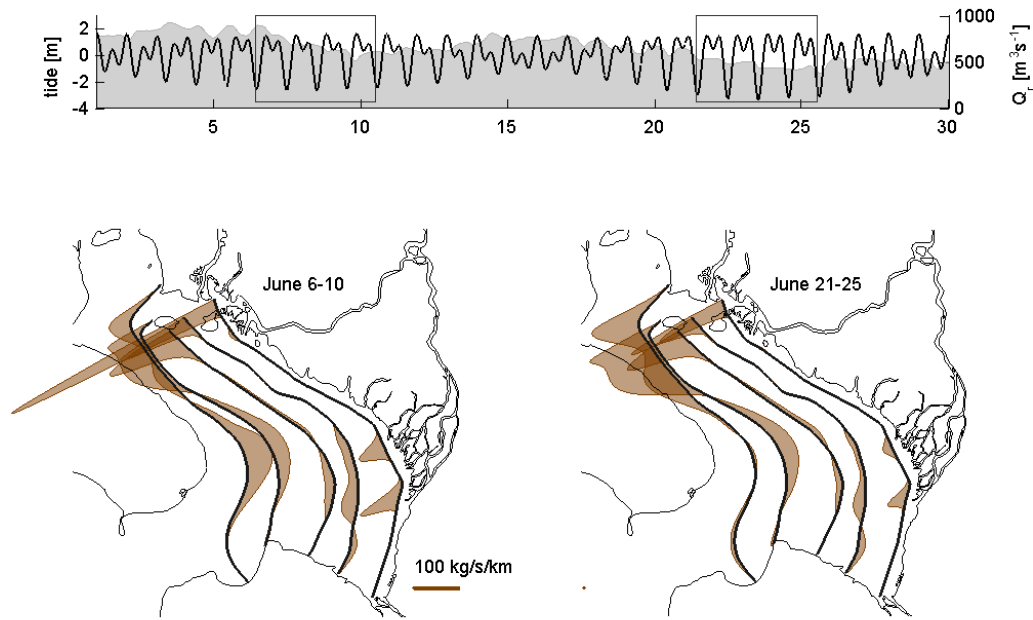


Figure 6. Maps of net sediment from the model. Sections are taken along isobaths and averaged over 4 diurnal tidal cycles (June 6-10 and June 21-25, 2009). Sediment flux is most intense offshore of the river mouths, and the flux across the tidal flats varies temporally with river discharge and spring-neap tidal forcing. Sediment is exported predominantly from the north fork where channelization and bed slopes are greater than in the south. Offshore sediment flux increased during the perigeon spring of June 21-25 due to extremely low tides that allow for longer periods of exposed channel flow, as well as due to decreased stratification with lower river discharge.

A fundamental question then is how the tidal variability in baroclinicity and stratification affects sediment transport across the tidal flats. Alternatively, is it necessary to resolve the density structure in these shallow environments to accurately simulation the sediment fluxes? The model results from the Skagit indicate that it is. The baroclinic forcing and stratification generated asymmetries in bottom stress and consequently in sediment transport. During flood tides, the baroclinic pressure gradient at the salinity front enhanced the bottom stress and during ebbs stratification suppressed turbulence and sediment resuspension. On the south Skagit flats, stratification was strongest and bottom stresses were weakest during neap tides (Figure 5). During spring tides stratification developed and persisted during weaker tides around high water, but maximum stresses occurred during the stronger diurnal tides.

An important distinction is that the transects shown in all but the bottom panel of Figure 5 follow one of the distributary channels flowing across the flats from the mouth of the south fork. At low tidal stage, river discharge continued to flow in the channel, and in the upper intertidal zone the channel experienced high seaward stresses due to river flow after the tide receded. In contrast, the lower flats remained inundated except for the most extreme low tides, and the stress asymmetry created by the baroclinic pressure gradient and the stratification remained flood dominant. We have quantified tidal stress asymmetry with the skewness, with positive values indicative of flood-dominant stresses. The lower channel was flood dominant, with the strength of the asymmetry increasing during neap tides, but the upper channel was ebb dominant due to the river flux. In contrast, a section on the flats near the channel (500 m to the north) shows that without the ebb-directed stresses of the river flow, the flats were even more flood dominant. This indicates that (1) stratification and baroclinic pressure gradient at the tidal salinity front enhanced stress asymmetry and consequently sediment trapping even in shallow water, and (2) that sediment transport in the distributary channels on the flats provided the primary means for sediment export, with the net flux dependent on tidal forcing and the river discharge.

Considering cross-flats slices alone would suggest that the stress asymmetry and sediment trapping at the salinity front would lead to significant sediment retention on the Skagit flats. However, bed sediment observations (by the Nittrouer group) suggest that relatively little fine sediment from the spring freshet was retained for long on the flats, and that instead much of the sediment was exported to the deeper basins to the south (Saratoga Passage) and north (Deception Pass). The realistic bathymetry and forcing of the model helps to resolve this discrepancy. Much of the observational effort discussed here focused on the broad southern Skagit flats with its network of small distributary channels. In contrast, the northern fork discharges over a much narrower intertidal region due to bathymetric constraints of Whidbey Island. The flats of the north fork are more channelized and have a steeper bed slope, and thus are more efficient at moving sediment seaward around low tide. Additionally, the combination of tidal rectification of the along-shore currents and tidal amplification that generates a pressure gradient between Saratoga Passage and Deception Pass produces a net northward flux on the flats, seen in both the observation and the model. This along-shore current provides a mechanism for moving sediment northward where it is efficiently moved into Whidbey Channel and out Deception Pass or into Saratoga Passage (Figure 6). The results demonstrate the importance of numerical modeling with realistic bathymetry, but constructing models with sufficient resolution to capture the necessary processes remains a challenge, as evidenced by the central role of the small distributary channels that were under-resolved by the model grid and available bathymetric data.

To extend our findings on frontal sediment trapping in the Skagit to other estuarine environments, we have recently examined bottom salinity fronts and sediment fluxes in model results from the Hudson River estuary. The Hudson is a much deeper (~15 to 40 m) and longer (~30 to 100 km) estuary than the Skagit, but despite the differences in scale we found similar processes of sediment trapping at distinct bottom salinity fronts due to gradients in stratification and baroclinic velocity. However, a key distinction between the two estuaries was that the fronts and associated sediment trapping in the Hudson occurred at multiple locations along the salinity gradient rather than a single interface between salty and fresh water. The fronts in the Hudson were topographically locked to transitions in estuary width or depth, and were spaced approximately one tidal excursion apart. This result provides a significant modification to the classic estuarine sediment transport paradigm of trapping that occurs predominantly in a single turbidity maximum located near the head of the salinity intrusion, or around 2 psu.

IMPACT/APPLICATIONS

Results from this project may be used to enhance morphological models of near river mouths, with applications to environmental assessment for the Navy. Trapping and deposition of sediment associated with density fronts could introduce spatial and temporal variability in bed consolidation and bathymetric relief on tidal flats. The project will also help to evaluate the skill of coastal hydrodynamic models at resolving density fronts, including the surface expressions that can be assessed with remote sensing. The importance of relatively subtle features like the distributary channels for net sediment flux in shallow, stratified flows provides guidance for the resolution needed for model domains and bathymetric data to adequately capture the dominant transport processes.

RELATED PROJECTS

The work here is closely linked to several other investigators in the Tidal Flats DRI. The field efforts on the Skagit were done in conjunction with Geyer and Traykovski. The model and grid development has been in collaboration with Geoff Cowles. Collaborations with others involved in the DRI include Raubenheimer and Elgar (for bathymetry, observations for model calibration, and use of the model to interpret water column and wind observations), Lerczak (model simulations at seasonal time scales), Signell and Sherwood (CSTM implementation), and Thomson and Chickadel (bathymetry). One post-doc (Nick Nidzieko at WHOI, currently at UMD Horn Point) and one student (Vera Pavel at WHOI) worked with Ralston on results from this modeling, although neither is directly funded by the project.

PUBLICATIONS

Nidzieko, NJ, and DK Ralston, 2012. Tidal asymmetry and velocity skew over tidal flats and shallow channels within a macrotidal river delta. *J. Geophys. Res.*, 117, C03001, 17 pp, doi:10.1029/2011JC007384. [published, refereed].

Ralston, DK, WR Geyer, PA Traykovski, and NJ Nidzieko, 2012. Effects of estuarine and fluvial processes on sediment transport over deltaic tidal flats, *Continental Shelf Res.*, doi:10.1016/j.csr.2012.02.004. [in press, refereed].

Ralston, DK, WR Geyer, and JC Warner, 2012. Bathymetric controls on sediment transport in the Hudson River estuary: lateral asymmetry and frontal trapping. *J. Geophys Res.*, [in press, refereed].

Raubenheimer, B., DK Ralston, S Elgar, D Giffen, and R Signell, 2012. Winds on the Skagit tidal flats, *Continental Shelf Research*, doi:10.1016/j.csr.2012.02.001. [in press, refereed].